Title: Effect of doping on nanoindentation induced incipient plasticity in InP crystal

Author: Dariusz Chrobak, Artur Chrobak, Roman Nowak

Citation style: Chrobak Dariusz, Chrobak Artur, Nowak Roman. (2019). Effect of doping on nanoindentation induced incipient plasticity in InP crystal. "AIP Advances" (2019, iss. 12, art. no. 125323, p. 1-6), doi 10.1063/1.5128784

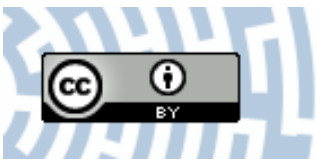

AIP Advances

Effect of doping on nanoindentation induced incipient plasticity in InP crystal

Cite as: AIP Advances **9**, 125323 (2019); https://doi.org/10.1063/1.5128784
Submitted: 23 September 2019 . Accepted: 24 November 2019 . Published Online: 23 December 2019

Dariusz Chrobak, Artur Chrobak, and Roman Nowak

Effect of doping on nanoindentation induced incipient plasticity in InP crystal

Cite as: AIP Advances 9, 125323 (2019); doi: 10.1063/1.5128784
Submitted: 23 September 2019 • Accepted: 24 November 2019 •
Published Online: 23 December 2019

Dariusz Chrobak,[1,a] Artur Chrobak,[2] and Roman Nowak[3]

AFFILIATIONS

[1] Department of Informatics and Materials Science, Institute of Materials Science, University of Silesia in Katowice, 75 Pułku Piechoty 1A, 41-500 Chorzów, Poland
[2] Department of Mathematics Physics and Chemistry, Institute of Physics, University of Silesia in Katowice, 75 Pułku Piechoty 1A, 41-500 Chorzów, Poland
[3] Nordic Hysitron Laboratory, Department of Chemistry and Materials Science, School of Chemical Engineering, Aalto University, Espoo 00076 Aalto, Finland

[a] dariusz.chrobak@us.edu.pl

ABSTRACT

This article is concerned with incipient plasticity in an InP crystal studied by nanoindentation experiments and *ab initio* simulations. We consider dislocation-nucleation phenomena and pressure-induced phase transformation to be the alternative mechanisms that govern the elastic-plastic transition displayed by the InP crystal. The *ab initio* calculations have shown that S- and Zn-doping of the low-pressure zinc blende structure of InP decreases the pressure of phase transformation of the rock-salt structure. The nanoindentation examination of undoped as well as S- and Zn-doped crystals of (001) and (111) orientation revealed an increase in contact pressure at the onset of plastic behavior (pop-in) for doped specimens. As they are contrary to the outcomes of the *ab initio* simulations, the results of nanoindentation experiments point toward dislocation nucleation as an origin of InP incipient plasticity. Additional investigations were performed on an undoped as well as Si-doped GaAs crystal, which showed that the contact pressure at the pop-in event takes a lower value for the Si-doped sample than the undoped sample. This result is in contrast to the case of the InP crystal displaying phase transformation-steered incipient plasticity of GaAs. Our investigations exhibit the complexity of the semiconductor's nanodeformation simultaneously providing a convenient way to identify its incipient plasticity mechanism.

Nanoindentation-induced incipient plasticity in initially dislocation-free crystal volume is reflected by the first discontinuity in the load-displacement (P-h) curve, which occurs when the indenter suddenly penetrates deeper into a material under a constant load. This effect, known as the pop-in, marks the onset of elastic-plastic transition. Such a pop-in is associated with the nucleation of dislocations as far as metallic crystals are concerned.[1–4] For semiconductors, however, the appearance of this specific singularity frequently involves structural phase transformations, as shown for nanoindentation deformed Si[5] or GaAs.[6–8] Interestingly, semiconductor nano-objects may deform plastically without phase transformations, which was demonstrated in Si nanowedges[9] and nanoballs,[10] as well as GaAs micropillars.[11] The effect of competition between phase transformation and dislocation-nucleation on elastic-plastic transition disclosed for Si and GaAs turned our attention to another semiconductor, namely, indium phosphide (InP). Due to its promising optoelectronic properties, the InP zinc blende crystal is used in a variety of electronic and optoelectronic devices (e.g., high-power and high-frequency electronics, solar cells, photodetectors, and photodiodes).[12] However, in order to extend the application range of InP in the field of microelectromechanical systems (MEMS), a deep understanding of InP mechanical properties is equally necessary.

The available experimental data stipulate the nucleation of dislocations as a cause of InP incipient plasticity. In fact, the investigations of the plastically deformed zone around the residual impression reveal complicated dislocation patterns,[13–18] while never disclosing the trace of structural phase transformation. Raman spectra

collected from a pristine surface and compared to these obtained at the center of an indent[17] serve as a good example of such research. Since the abovementioned structural investigations were carried out after nanoindentation experiments, we are convinced that it is premature to exclude the effect of phase transformation on the nanoindentation-induced elastic-plastic transition in the InP crystal.

In order to determine the mechanism that leads to the initiation of plastic deformation in nanoindented InP, we anticipated the doping-dependence of incipient plasticity because the presence of an admixture in a crystal lattice may affect both phase transformations and dislocations nucleation. In fact, the phase transformation from a zinc blende (zb) to a rock-salt (rs) structure in the InP crystal doped by Fe occurs at a pressure of 8.4 GPa,[19] which is significantly lower than the transformation pressure of undoped InP (9.8–13 GPa, see Refs. 20–22), which is well in line with the results obtained for Se-doped InP.[23] Furthermore, the doping of InP causes an increase in microhardness[24] and yield stress[25,26] and it suppresses the generation of dislocations during crystal growth.[27,28] Consequently, the presence of dopants in the lattice of the InP crystal should increase the shear stress required for the dislocation to nucleate. In other words, if the elastic-plastic transition is caused by the nucleation of dislocations, the doping of InP should increase the contact pressure at the pop-in, while an opposite effect is expected to occur when the elastic-plastic transition is governed by structural phase transformation.

In this study, we present nanoindentation experiments, supported by *ab initio* quantum calculations, carried out on undoped and doped InP crystals with different crystallographic orientations. For the sake of comparison, the output of our research also contains the findings regarding the doping effect of GaAs, which is in contrast to the case of InP.

Load-controlled nanoindentations (Triboindenter TI-950) were carried out using a conical diamond probe with a spherical tip. The experiments were performed on an undoped and doped InP crystal surface of (001) and (111) crystallographic orientation, respectively, fabricated by the vertical gradient freeze method. Additional measurements of undoped and Si-doped (001) GaAs crystals were performed for the sake of comparison. The carrier concentrations (n) of the doped InP crystals are shown in Table I, while this parameter is in the range 7.2–11.7 × 10^{17} cm^{-3} for Si-doped GaAs. Since the dislocation etch pit density was lower than 4000 cm^{-2} (approximate distance between dislocations is ~150 μm), the experiments with a sharp indenter would be capable of probing both elastic and plastic properties of investigated crystals within virtually dislocation-free nanovolume. The experiments were carried out under a maximum load of 5 mN and 6 mN for InP and GaAs, respectively. The used load function consisted of 5 s loading and an equally long unloading path, with a dwell time of 2 s.

The *ab initio* quantum simulations were performed with the Quantum Espresso code.[29] The ultrasoft pseudopotentials[30] and Perdew-Burke-Ernzerhof exchange-correlation functional[31] were used. In order to achieve highly accurate calculations, the states of valence electrons were expanded into a series of plane waves with a kinetic energy cut-off of 80 Ry. Furthermore, the first Brillouin zone was sampled with the 13 × 13 × 13 Monkhorst-Pack mesh.[32] The effect of doping on the equilibrium pressure (p_e) of zinc blende and rock-salt phases was studied using a supercell composed of 2 × 2 × 2 unit cells in which the central atom was replaced by an admixture. The relaxation of atomic positions was carried out until the interatomic forces were less than 1.0 × 10^{-5} Ry/a.u.^{3}. The modeled concentration of admixtures (6.3 × 10^{20} cm^{-3}, InP lattice constant a = 5.869 Å) was higher than the one of our samples (~10^{18} cm^{-3}). Simulation of real dopant concentration required the employment of a supercell consisting of approximately 10 × 10 × 10 unit cells with 8000 atoms. Such a large number of atoms causes very high consumption of computational resources and therefore forced us to search for a qualitative approach based on a smaller supercell.

The *ab initio* calculations for zinc blende and rock-salt phases of the undoped InP crystal resulted in the lattice constants a_{zb} = 5.829 Å and a_{rs} = 5.418 Å and the bulk moduli B_{zb} = 70.5 GPa and B_{rs} = 88.8 GPa, which are in agreement with the data available in the literature,[33] giving credit to the accuracy of our calculations. However, the most significant result concerns the changes in enthalpy with pressure calculated for undoped, Zn-doped, and S-doped lattices. Figure 1(a) shows that an equilibrium pressure of p_e = 8.4 GPa was obtained for the undoped crystal; although a bit lower than the experimental value of 9.8 GPa,[22] it does agree well with the earlier reported *ab initio* data.[33] The modeling of the zinc blende and rock-salt structure of doped InP was performed using a 2 × 2 × 2 supercell in which indium was replaced by zinc, (In, Zn)P, while phosphorus was replaced by sulfur, In(P, S). This method of atom substitution was dictated by the atom size analysis and the present *ab initio* calculations (refer to the supplementary material). The equilibrium pressure p_e obtained for (In, Zn)P is 7.1 GPa [Fig. 1(b)], while the case of In(P, S) led us to a slightly higher value of 7.4 GPa [Fig. 1(c)]. These results show that the presence of sulfur as well as zinc atoms in the InP crystal lattice reduces the equilibrium pressure between the zinc-blend and rock-salt phases. Hence, it is reasonable to expect that this particular doping decreases the pressure of the structural phase transformation in InP.

Numerous nanoindentation experiments were performed on undoped and doped InP crystals to conclude on the origin of the

TABLE I. The carrier concentration (n), the reduced Young's modulus (E_r) and the pop-in mean contact pressure (p_m) measured for various oriented InP crystals.

	(001)			(111)		
InP	Undoped	S-doped	Zn-doped	Undoped	S-doped	Zn-doped
n (cm^{-3})	3.7–6.5 × 10^{15}	1.7–1.9 × 10^{18}	3.1–3.4 × 10^{18}	3.8–4.3 × 10^{15}	3.2–3.7 × 10^{18}	4.3–4.9 × 10^{17}
E_r (GPa)	62.5 ± 0.9	68.6 ± 0.4	67.3 ± 0.6	72.4 ± 0.6	77.8 ± 0.6	76.2 ± 0.5
p_m (GPa)	7.6 ± 0.4	8.2 ± 0.3	8.0 ± 0.4	7.5 ± 0.3	7.8 ± 0.3	7.9 ± 0.2

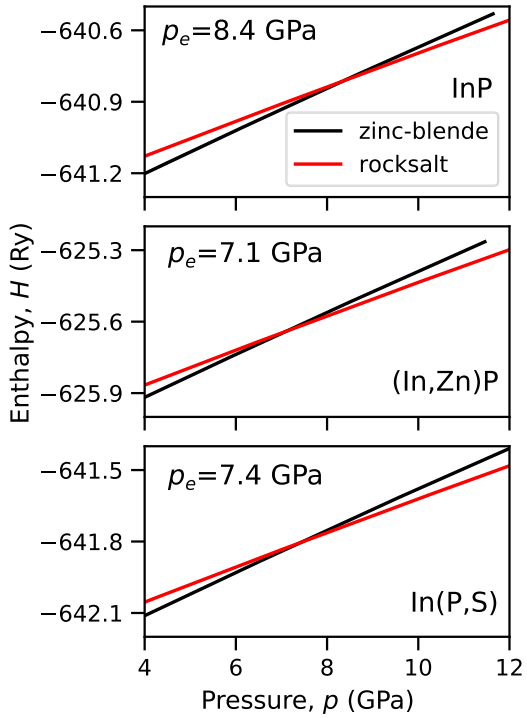

FIG. 1. The effect of pressure on the enthalpy H = E + pV calculated for zinc blende (black) and rock-salt (red) phases of the undoped as well as S- and Zn-doped InP crystal. The equilibrium pressure for the zinc blende and rock-salt phases refers to the point where the H(p) curves intersect.

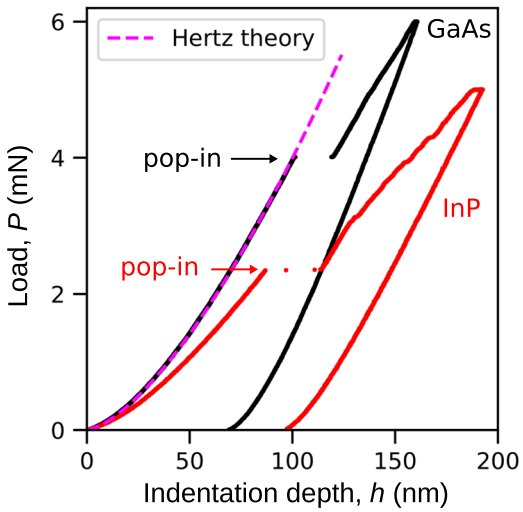

FIG. 2. Typical result of the nanoindentation experiment obtained for undoped GaAs (black) and InP (red) crystals. The dashed (magenta) curve represents the Hertz fit to the P-h curve of the reference undoped GaAs crystal. The arrow indicates the pop-in event that marks the onset of nanoindentation-induced plastic deformation.

InP plasticity (approx. 400 P-h curves were registered for each sample). We based the pertinent analysis of nanoindentation data on the equations derived from the Hertz theory of elastic contact between the sphere and isotropic half-space, $P(h) = (4/3)E_rR^{1/2}h^{2/3}$ and $a^2 = Rh$, where P is the indenter load, h refers to the indenter displacement, R indicates the spherical indenter tip radius, a is the radius of the contact area, and E_r is the reduced Young's modulus.[34] The tip radius R = 1178 ± 12 nm was estimated using the undoped GaAs crystal by fitting the load-displacement function P(h) to 100 nanoindentation P-h curves [Fig. 2]. This procedure employed the reduced Young's modulus of 87.2 GPa, calculated using GaAs and diamond indenter elastic constants.[35] Furthermore, assuming the indenter tip radius R is known, the reduced Young's modulus and the contact pressure at the onset of elastic-plastic transition (pop-in) in InP crystals were calculated as $p_c = 2/3(6P_cE_r^2/(\pi^3R^2))^{1/3}$, where P_c is the load at the pop-in.[34] We found higher E_r values for doped samples and obtained values given in Table I with the (111) indentation surface. It is worth noting that inaccuracy in evaluation of the contact pressure of the individual pop-in results from the uncertainty of the tip radius ΔR measurement by the formula $\Delta p_c = P\Delta R/(\pi R^2 h)$. For example, the pop-in contact pressure of 10.7 GPa for the P-h curve of GaAs (Fig. 2) was determined with an accuracy of 0.1 GPa. The inaccurate estimation of load and displacement affects p_c to a less extent, namely, at the second decimal place.

The contact pressure distributions obtained for undoped, S-doped, and Zn-doped InP crystals are presented in the form of histograms (Fig. 3 and 4), for which the bin width (0.156 GPa) was optimized using the method described in Ref. 36. There is a systematic shift in the contact pressure distributions of doped InP towards higher values (see Table I for the values of the mean contact pressures as well as their variances). In order to discuss the above result, we estimated the initial (critical) radius of the stable dislocation loop r_c and then compared it with the approximate distance between the dopants. The description of dislocations will be simplified within the framework of the linear theory of elasticity that predicts the critical shear stress for the nucleation of dislocation loops, $\tau_c = (2 - \nu)Gb/[(1 - \nu)4\pi r_c]$, where $r_c = r_0e^3/4$, r_0 is the dislocation core radius, and b is the length of Burger's vector of dislocation.[37,38] We used the Voigt effective shear modulus, G = 36.4 GPa, and Poisson's ratio, ν = 0.29, which were calculated using the following elastic constants of the InP crystal: c_{11} = 101.1 GPa, c_{12} = 56.1 GPa, and c_{14} = 45.6 GPa.[35] Moreover, estimation of the critical radius of dislocation loops requires the shear stress to be resolved in an active slip system. Here, as an illustration, we will consider the case of indentation along the [111] direction and the [101] (111) slip system. It can be shown that for the selected slip system, the maximum resolved shear stress $\tau = 0.544(\tau_1)_{max}$,[39] where the relationship between maximum shear stress and contact pressure comes from the Hertz theory of elastic contact, $(\tau_1)_{max} = 0.48p_c$ (see the supplementary material). Now, applying the data presented in Table I, the value of τ for the undoped crystal becomes1.96 GPa from which the critical radius of the dislocation loop can be calculated, $r_c = 3.6b$. Taking into account Burger's vector of perfect dislocation a/2[110] (a = 0.5869 nm[35] and b = 0.42 nm), the diameter of the dislocation loop of the critical size is equal to 3 nm, which is of the same order as the approximate distance between admixture atoms that varies from 8.4 nm to 6.8 nm (for a carrier concentration of 3.2–4.9 × 10^{18} cm^{-3}).

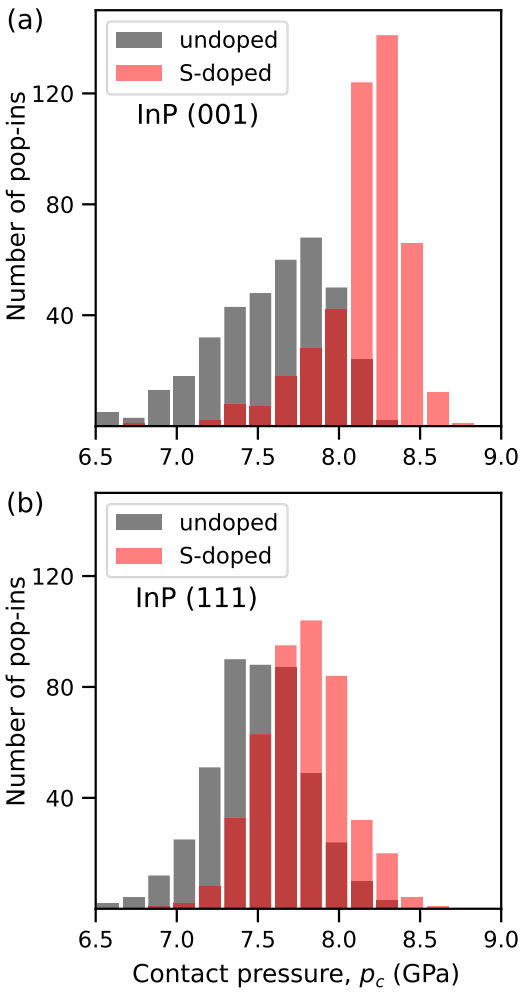

FIG. 3. The histogram analysis showing the relationship between the number of pop-in events and their contact pressures p_c. Indentations were performed along the (a) [001] and (b) [111] crystallographic axis of the undoped as well as S-doped InP crystal.

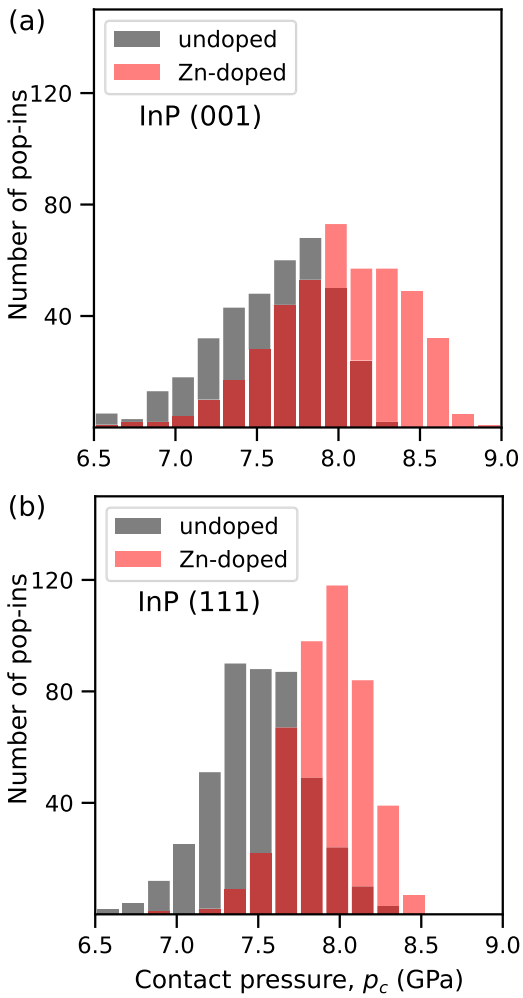

FIG. 4. The histogram analysis showing the relationship between the number of pop-in events and their contact pressures p_c. Indentations were performed along the (a) [001] and (b) [111] crystallographic axis of the undoped as well as Zn-doped InP crystal.

The above analysis shows that the activity of dislocations at the onset of the elastic-plastic transition can be affected by their interaction with the point defects. The resulting pinning effect enhances the critical shear stress required to move the dislocation from the impurity atoms. To justify the pinning effect, let us assume L to be the average distance between point defects. In order to break away the dislocation from the impurities, the shear stress σ_c that should be applied is inversely proportional to the average distance L between the point defects, $\sigma_c \sim 1/L$ (see the supplementary material). Thus, the stress ratio σ_{c1}/σ_{c2} assumes the form $\sigma_{c1}/\sigma_{c2} \approx L_2/L_1$, where the lower indices reflect a different doping level. This means that an increase in dopant concentration (decrease in the L value) raises the stress necessary to unpin the dislocation. This outcome agrees with the observation that doping decreases the density of dislocations during the growth of InP and it inhibits the mobility of dislocations in a stressed crystal. Consequently, the observed increase in the pop-in contact pressure (Table I and Figs. 3 and 4) can be understood in terms of nucleation and development of the dislocation net but not the phase transformation for which a decrease in the pop-in contact pressure is expected from our *ab initio* simulations.

In order to show the complexity of nanoindenation-induced incipient plasticity in the semiconductor world, we carried out additional experiments on an undoped and Si-doped GaAs crystal. It is known that nanoindentation induced plastic deformation of the GaAs crystal is initiated by the phase transformation from a zinc blende to a rock-salt-like structure (space group Cmcm).[7,8] Given that Si doping decreases the pressure of GaAs phase transformation,[40,41] the pop-in pressure distribution of doped-GaAs should be shifted toward lower pressure. Indeed, this effect was confirmed by the present experiments as the analysis of nanoindentation results (Fig. 5) shows the expected shift in pop-in pressure distribution associated with a slight decrease in contact pressure from 11.1

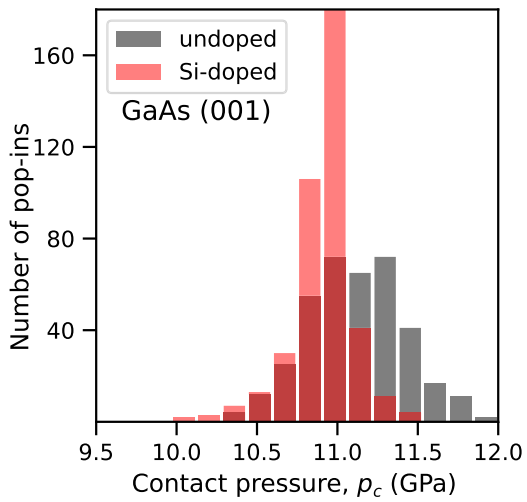

FIG. 5. The histogram analysis of the pop-in phenomenon showing the relationship between the number of pop-in events and their contact pressure p_c performed on the (001) surface of the undoped and Si-doped GaAs crystal. The registered decrease in the contact pressure distribution is in contrast to the phenomenon observed for InP.

± 0.4 GPa to 10.9 ± 0.2 GPa. The reason for different origins of nanoindentation-induced incipient plasticity in InP and GaAs, although confirmed by our experiments, is unknown and requires further investigations.

In summary, the nanoindentation examination of the undoped and doped InP crystals revealed an increased contact pressure at the onset of the plastic deformation in the doped materials. This effect led to our conclusions on the dislocations nucleation-steered mechanism of incipient plasticity of the InP crystal. We discussed the role of the pinning effect as a potential cause of the observed mechanical behavior of the InP crystal. The output of our considerations and experiments is in contrast to the results of the experiments performed for GaAs for which phase transformation governed elastic-plastic transition is expected. In conclusion, we would like to indicate that our study presents a convenient way to identify the mechanism of incipient plasticity for semiconducting crystals.

See the supplementary material for nanoindentation data, a short discussion of InP doping based on *ab initio* simulations and comments on the pinning effect.

The authors acknowledge support from the National Science Centre, Poland (Grant No. 2016/21/B/ST8/02737), as well as the CSC-IT Center for Science (Finland) for computational resources. RN acknowledges the Department of Chemistry and Materials Science for overall support.

REFERENCES

[1] S. G. Corcoran, R. J. Colton, E. T. Lilleodden, and W. W. Gerberich, Phys. Rev. B **55**, R16057 (1977).
[2] C. A. Schuh, J. K. Mason, and A. C. Lund, Nat. Mater. **4**, 617 (2005).
[3] K. Jurkiewicz, M. Pawlyta, D. Zygadło, D. Chrobak, S. Duber, R. Wrzalik, A. Ratuszna, and A. Burian, J. Mater. Sci. **53**, 3509 (2018).
[4] I. Szlufarska, A. Nakano, and P. Vashista, Science **309**, 911 (2005).
[5] Y. B. Gerbig, C. A. Michaels, A. M. Forster, and R. F. Cook, Phys. Rev. B **85**, 104102 (2012).
[6] R. Abram, D. Chrobak, and R. Nowak, Phys. Rev. Lett. **118**, 095502 (2017).
[7] D. Chrobak, K. Nordlund, and R. Nowak, Phys. Rev. Lett. **98**, 045502 (2007).
[8] R. Nowak, D. Chrobak, S. Nagao, D. Vodnick, M. Berg, A. Tukiainen, and M. Pessa, Nat. Nanotechnol. **4**, 287 (2009).
[9] D. Ge, A. M. Minor, E. A. Stach, and J. W. Morris, Philos. Mag. **86**, 4069 (2006).
[10] D. Chrobak, N. Tymiak, A. Beaber, W. W. Gerberich, and R. Nowak, Nat. Nanotechnol. **6**, 480 (2011).
[11] J. Michler, K. Wasmer, S. Meier, F. Ostlund, and K. Leifer, Appl. Phys. Lett. **90**, 043123 (2007).
[12] N. P. Siwak, X. Z. Fan, and R. Ghodssi, J. Micromech. Microeng. **25**, 043001 (2015).
[13] E. Le Bourhis, J. P. Riviere, and A. Zozime, J. Mater. Sci. **31**, 6571 (1996).
[14] G. Patriarche and E. Le Bourhis, J. Mater. Sci. **36**, 1343 (2001).
[15] K. Wasmer, R. Gassilloud, J. Michler, and C. Ballif, J. Mater. Res. **27**, 320 (2012).
[16] C. M. Almeida, R. Prioli, Q. Y. Wei, and F. A. Ponce, J. Appl. Phys. **112**, 063514 (2012).
[17] S. R. Jian and J. S. C. Jang, J. Alloys Compd. **482**, 498 (2009).
[18] Y. J. Chiu, S. R. Jian, T. J. Liu, P. H. Le, and J. Y. Juang, Micromachines **9**, 611 (2018).
[19] C. M. Lin, I. J. Hsu, S. C. Lin, Y. C. Chuang, and J. Y. Juang, Sci. Rep. **8**, 1284 (2018).
[20] C. S. Menoni and I. L. Spain, Phys. Rev. B **35**, 7520 (1987).
[21] R. J. Nelmes and M. I. McMahon, Semicond. Semimetals **54**, 145 (1998).
[22] A. Mujica, A. Rubio, A. Munoz, and R. J. Needs, Rev. Mod. Phys. **75**, 863 (2003).
[23] D. N. Bose, B. Seishu, G. Parthasarathy, and E. S. R. Gopal, Proc. R. Soc. London, Ser. A **405**, 345 (1986).
[24] D. Arivuoli, R. Fornari, and J. Kumar, J. Mater. Sci. Lett. **10**, 559 (1991).
[25] D. Brasen and W. A. Bonner, Mater. Sci. Eng. **61**, 167 (1983).
[26] I. Yonenaga and K. Sumino, J. Appl. Phys. **74**, 917 (1993).
[27] P. J. Roksnoer and M. M. B. van Rijbroek-van den Boom, J. Cryst. Growth **66**, 317 (1984).
[28] O. Oda, K. Katagiri, K. Shinohara, S. Katsura, Y. Takahashi, K. Kainosho, K. Kohiro, and R. Hirano, Semicond. Semimetals **31**, 93 (1990).
[29] P. Giannozzi *et al.*, J. Phys.:Condens.Matter **29**, 465901 (2017).
[30] A. Dal Corso, Comput. Mater. Sci. **95**, 337 (2014).
[31] J. P. Perdew, K. Burke, and M. Ernzerhof, Phys. Rev. Lett. **77**, 3865 (1996).
[32] H. J. Monkhorst and J. D. Pack, Phys. Rev. B **13**, 5188 (1976).
[33] O. Arbouche, B. Belgoumène, B. Soudini, Y. Azzaz, H. Bendaoud, and K. Amara, Comput. Mater. Sci. **47**, 685 (2010).
[34] K. L. Johnson, *Contact Mechanics* (Cambridge University Press, Cambridge, 1985).
[35] See http://www.ioffe.ru/SVA/NSM/Semicond/ for about the elastic constants of GaAs.
[36] H. Shimazaki and S. Shinomoto, Neural Comput. **19**, 1503 (2007) .
[37] H. S. Leipner, D. Lorenz, A. Zeckzer, H. Lei, and P. Grau, Physica B **308-310**, 446 (2001).
[38] D. Lorenz, A. Zeckzer, U. Hilpert, P. Grau, H. Johansen, and H. S. Leipner, Phys. Rev. B **67**, 172101 (2003).
[39] Y. L. Chiu and A. H. W. Ngan, Acta Mater. **50**, 1599 (2002).
[40] D. Chrobak, K. H. Kim, K. J. Kurzydowski, and R. Nowak, Appl. Phys. Lett. **103**, 072101 (2013).
[41] D. Chrobak, J. Raisanen, and R. Nowak, Scr. Mater. **102**, 31 (2015).